Table 3 Extremes of variations on the standard interception

P	PL	ML	PH	MH	%
SR	50	6.612	1000	132.010	1897
TM	80	3.932	500	599.756	15153
AS	4.75	39.398	0.25	39.674	0.70
AI	60/300	39.646	180	39.685	0.10
AF	315	39.398	75	40.723	3.36
RM	−250	6.615	0	39.648	499
IM	250	33.503	0	39.648	18
CM	250	8.981	0	39.648	341

[a]Key: P = parameter varied (mnemonics correspond to Table 2), PL/PH = parameter value that resulted in the smallest/largest maneuver (units as in Table 2), ML/MH = size of maneuver in m/s corresponding to PL/PH, % = difference between ML and MH expressed as a percentage of ML.

increased linearly as threat radius increased, and increased approximately exponentially as maneuver interval shrank. One surprising result was the small effect of variations in the interceptor's velocity, which altered the size of the evasive maneuver by only a few percent. Errors in the radial and cross-track directions resulted in nearly linear reductions in the size of the required maneuver. Errors in in-track miss distance produced a more gradual drop-off in maneuver size.

Summary and Suggestions for Further Work

A threat sphere moving in a Keplerian orbit was used to model an attack on a satellite. Defeat of the attack was considered by changing the satellite's orbital velocity at a specified time to avoid penetration of the threat sphere. An algorithm using a method of differential corrections was developed to find the minimum-impulse evasive maneuver. A 45 deg inclination impulsive direct ascent attack on a geosynchronous satellite with a threat sphere radius of 300 km and a maneuver time about 2 h before the nominal impact time was used as a reference case. The optimal evasive maneuver had a velocity change of 39.648 m/s with a nonzero out-of-plane component. The sensitivity of this solution to variations in intercept parameters was also studied. Maneuver time was the most important parameter, followed by threat sphere radius. In every case no more than two locally optimal solutions were found.

Further study of orbital evasive maneuvers along the lines drawn here might include the effects of uncertainty, improvement of accuracy of the model, and consideration of methods of jointly optimizing evasive maneuver size and other relevant factors. The algorithm used here takes no account of uncertainties in the data, either in knowledge of the state vectors or in the precision with which a recommended maneuver can be made. In reality these uncertainties might be significant. In the area of improving the fidelity of the model there are three interesting possibilities: non-Keplerian dynamics, nonimpulsive maneuvers, and nonspherical threat volumes (e.g., the acquisition cone of a radar). Perhaps the most important area of study is the optimization of other things along with impulse size. Such things as predictability, required attitude changes, and the return to the mission orbit might be significant factors in selecting an evasive maneuver. The best maneuver in a given situation will be determined by considering all of these factors.

References

[1]Prussing, J. E. and Heckathorn, W. G., "Optimal Impulsive Time-fixed Direct-ascent interception," AAS/AIAA Astrodynamics Specialists Conference, Paper AAS 85-437, Vail, CO, Aug. 1985.

[2]Burk, Roger C., "Minimum Impulse Orbital Evasive Maneuvers," M.S. Thesis, Air Force Inst. of Technology, Wright-Patterson AFB, OH, 1985.

[3]Escobal, P. R., *Methods of Orbit Determination*, 2nd ed., Wiley, New York, 1965; reprinted by Robert E. Krieger Publishing, Malabar, FL, 1985, Chap. 9.

Method for Stability Analysis of an Asymmetric Dual-Spin Spacecraft

Hai Xing Yang*
Shanghai Jiao-Tong University,
Shanghai, China

Introduction

A DUAL-SPIN spacecraft may be approximately modeled as a gyrostat. Leimanis,[1] Kane,[2] Cochran,[3] and Tsuchiya[4] have each provided the analytical solution or nutational stability for the attitude motion of an axisymmetric or asymmetric gyrostat by use of Euler's equations. In this paper, first-order differential equations with variables, the Euler angles, and the angle of relative rotation are derived instead of Euler's equations.[5] From the first-order equations, the nutational stability and the criteria for stable quasipermanent spin are directly determined. The behavior of unstable attitude motion is investigated with the aid of the energy integral of the system.

First-Order Equations of Motion

The dual-spin spacecraft S consists of rigid bodies A and B connected by a bearing axis (see Fig. 1). A^*, B^*, and S^*, the respective mass centers of A, B, and S, lie on the bearing axis. The distance between A^* and B^* is 1. Body A is an asymmetric rotor. Its centroidal principal axis system is $(A^* - X_1X_2X_3)$. Body B is an axisymmetric platform. Its axis of symmetry is aligned with the X_1-axis. The $(B^* - X_1Y_2Y_3)$ system is fixed in body B, the orientation of which relative to $(B^* - X_1X_2X_3)$ is specified by the angle α. Bodies A and B and system S have masses m_A, m_B, and m, respectively. Their individual centroidal inertia dyadics $\boldsymbol{A}$, $\boldsymbol{B}$, and $\boldsymbol{I}$ are

$$\boldsymbol{A} = \sum_{i=1}^{3} A_i \boldsymbol{x}_i \boldsymbol{x}_i, \quad \boldsymbol{B} = \sum_{i=1}^{3} B_i \boldsymbol{x}_i \boldsymbol{x}_i, \quad \boldsymbol{I} = \sum_{i=1}^{3} I_i \boldsymbol{x}_i \boldsymbol{x}_i \tag{1}$$

$$I_1 = A_1 + B_1, \quad I_i = A_i + B_3 + l^2 m_A m_B / m \ (i = 2, 3) \tag{2}$$

where $\boldsymbol{x}_i$ are unit vectors parallel with axis X_i ($i = 1, 2, 3$).

Establish $(S^* - Z_1Z_2Z_3)$, the coordinate system of angular momentum, with Z_1-axis along the angular momentum vector of system S about S^*. Let ψ, ϑ and φ be Euler angles of the centroidal principal axis system $(S^* - X_1X_2X_3)$ relative to $(S^* - Z_1Z_2Z_3)$ (see Fig. 2). Since there is no external torque, the rotational angular momentum of the system is constant. It may be expressed in the form

$$\boldsymbol{H} = Hc\vartheta \boldsymbol{x}_1 + Hs\vartheta s\varphi \boldsymbol{x}_2 + Hs\vartheta c\varphi \boldsymbol{x}_3 \tag{3}$$

Here H is the magnitude of $\boldsymbol{H}$ and is a first integral; $c(\ )$ and $s(\ )$ are defined as $\cos(\ )$ and $\sin(\ )$, respectively, for convenience. According to its definition, $\boldsymbol{H}$ may also be written as

$$\boldsymbol{H} = \boldsymbol{I} \cdot \boldsymbol{\omega} + \boldsymbol{B} \cdot \boldsymbol{\Omega} \tag{4}$$

where $\boldsymbol{\Omega}$ and $\boldsymbol{\omega}$ are the angular velocity of B relative to A and of A, respectively, which may be expressed as

$$\boldsymbol{\Omega} = \Omega \boldsymbol{x}_1 \tag{5a}$$

$$\boldsymbol{\omega} = \sum_{i=1}^{3} \omega_i \boldsymbol{x}_i \tag{5b}$$

Received Nov. 6, 1986; revision received Jan. 7, 1986.

*Assistant Professor, Department of Engineering Mechanics.

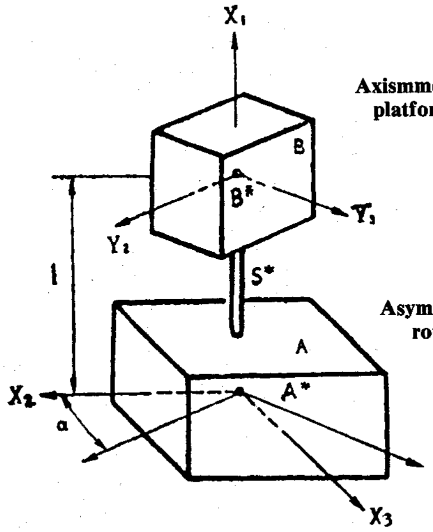

Fig. 1 Spacecraft model.

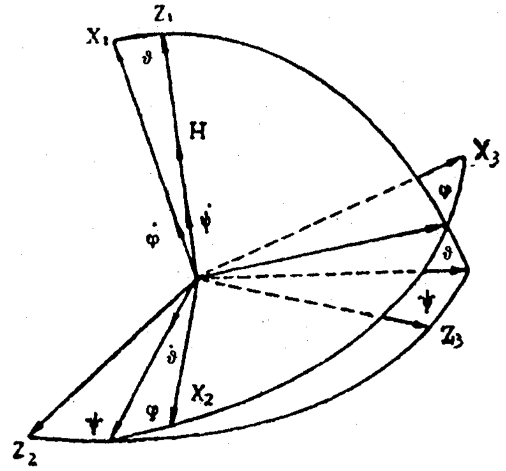

Fig. 2 Euler angles.

The angular momentum and the principle of angular momentum of body B about B^* may be expressed as

$$H_B \doteq B \cdot (\omega + \Omega) \tag{6}$$

$$\tilde{d}H_B/dt + \omega \times H_B = Mx_1 \tag{7}$$

where the superscript $\sim$ means that the derivative is in ($B^* - X_1X_2X_3$), and M represents despun-motor torque applied to B about the X_1-axis, which is the sum of motor and friction torques. The component of Eq. (7) along the X_1-axis is

$$B_1(\dot{\omega}_1 + \dot{\Omega}) = M \tag{8}$$

If there is no external torque, then

$$\omega_1 + \Omega = \Gamma \tag{9}$$

Here, Γ is also an integral of the motion. Equation (9) shows that the component of the angular momentum of body B along the X_1-axis is conservative.

Let $\nu = H/I$, $\lambda = I_3/A_1$, $\rho = I_3/I_2$, and $\mu = B_1/A_1$. From the identities of Eqs. (3) and (4), the components of angular velocity of body A are given by

$$\omega_1 = \lambda\nu c\vartheta - \mu\Gamma, \qquad \omega_2 = \rho\nu s\vartheta s\varphi, \qquad \omega_3 = \nu s\vartheta c\varphi \tag{10}$$

From geometry (see Fig. 2), we have the kinematic equations

$$\dot{\vartheta} = \omega_2 c\varphi - \omega_3 s\varphi \tag{11a}$$

$$\dot{\psi} = (\omega_2 s\varphi + \omega_3 c\varphi)/s\vartheta \tag{11b}$$

$$\dot{\varphi} = \omega_1 - (\omega_2 s\varphi + \omega_3 c\varphi)\cot\vartheta \tag{11c}$$

By substituting Eqs. (9) and (10) into Eq. (11), and noting $\dot{\alpha} = \Omega$, it follows that

$$\dot{\vartheta} = \nu(\rho - 1)\, s\vartheta s\varphi c\varphi \tag{12a}$$

$$\dot{\psi} = \nu[1 + (\rho - 1)s^2\varphi] \tag{12b}$$

$$\dot{\varphi} = \nu c\vartheta[\lambda - 1 - (\rho - 1)s^2\varphi] - \mu\Gamma \tag{12c}$$

$$\dot{\alpha} = (1 + \mu)\Gamma - \lambda\nu c\vartheta \tag{12d}$$

The above first-order differential equations in the variables ψ, ϑ, φ, and α determine the attitude motion of a torque-free, asymmetric dual-spin spacecraft.

Nutational Stability

On the right-hand side of Eq. (12), φ is generally a "fast" variable and ϑ is a "slow" variable. By applying the averaging algorithm with a period of $\pi/\dot{\varphi}$ to Eq. (12), one finds that

$$\dot{\bar{\vartheta}} = 0, \ \bar{\vartheta} = \vartheta_0 \tag{13a}$$

$$\dot{\bar{\psi}} = \nu(\rho + 1)/2 \tag{13b}$$

$$\dot{\bar{\varphi}} = \nu c\vartheta_0[\lambda - (\rho + 1)/2] - \mu\Gamma \tag{13c}$$

$$\dot{\bar{\alpha}} = (1 + \mu)\Gamma - \lambda\nu c\vartheta_0 \tag{13d}$$

where variables with the bar are "averaged" variables. It is obvious that $\dot{\bar{\vartheta}}$, $\dot{\bar{\psi}}$, $\dot{\bar{\varphi}}$, and $\dot{\bar{\alpha}}$ are all constants. It is a quasiregular precession. If $\vartheta_0 = 0$, then it is a quasipermanent spin about X_1-axis. Now one finds that $\bar{\omega}_1$ is also a constant from Eq. (10a)

$$\bar{\omega}_1 = \lambda\nu c\vartheta_0 - \mu\Gamma \tag{14}$$

When the spin angular velocity of the rotor becomes near zero, i.e., the case for Eq. (6) in Ref. 4, the above quasiregular precession or quasipermanent spin may be unstable. By substituting ω_1 of Eq. (10) into Eq. (12c), one arrives at

$$\dot{\varphi} = -(\omega_1 + \mu\Gamma)\left[\left(\frac{\rho + 1}{2\lambda} - \frac{1}{1 + \mu\Gamma/\omega_1}\right) - \left(\frac{\rho - 1}{2\lambda}\right)c2\varphi\right] \tag{15}$$

The process of averaging requires that $|\dot{\varphi}| \neq 0$. If the solution is satisfied $|\dot{\varphi}| > 0$, then one must have

$$\left(\frac{\rho + 1}{2\lambda} - \frac{1}{1 + \mu\Gamma/\omega_1}\right)^2 > \left(\frac{\rho - 1}{2\lambda}\right)^2 \tag{16}$$

The condition in Eq. (16) is the same as the condition in Eq. (19) in Ref. 4. Either of these may be replaced by

$$\Gamma/\omega_1 > \max(F_1, F_2) \text{ or } \Gamma/\omega_1 < \min(F_1, F_2)$$

$$F_1 = (I_3 - A_1)/B_1 \quad F_2 = (I_2 - A_1)/B_1 \tag{17}$$

Behavior of Attitude Motion

In order to further investigate the behavior of attitude motion as a result of asymmetry of body A, one can directly use the kinetic integral of the system. In the case of zero

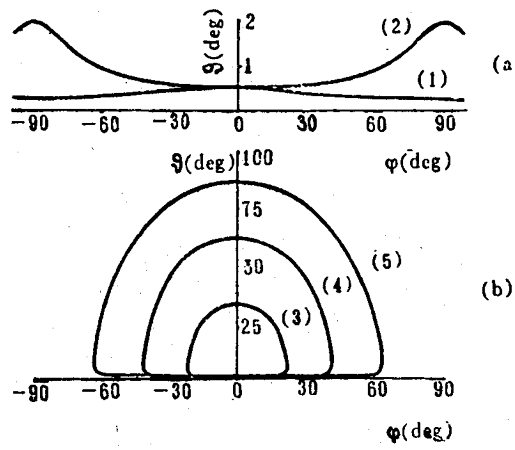

Fig. 3 Trajectories in $\varphi - \vartheta$ plane.

despun-motor torque, the kinetic energy is conservative.

$$T = (½)\ \omega \cdot \boldsymbol{I} \cdot \omega + \boldsymbol{\Omega} \cdot \boldsymbol{B} \cdot \omega + (½)\ \boldsymbol{\Omega} \cdot \boldsymbol{B} \cdot \boldsymbol{\Omega} = \text{const} \tag{18}$$

So, besides H and Γ, another first integral σ can be expressed as

$$\sigma = (2T - B_1\Gamma^2)/I_3\nu^2 = (A_1\omega_1^2 + I_2\omega_2^2 + I_3\omega_3^2)/I_3\nu^2 \tag{19}$$

Putting Eq. (10) into the above equation and letting $\Gamma/\nu = k$, one arrives at

$$\sigma = (\lambda c\vartheta - \mu k)^2/\lambda + s^2\vartheta[1 + (\rho - 1)s^2\varphi] \tag{20}$$

The integral σ can be determined in terms of the initial values ϑ_0, φ_0, Γ_0, and ω_{10}. The system parameters for a dual-spin spacecraft example are as follows:

$$I_1 = 480 \text{ kgm}^2 \quad I_2 = 360 \text{ kgm}^2$$

$$I_3 = 440 \text{ kgm}^2 \quad B_1 = 160 \text{ kgm}^2$$

$$\vartheta_0 = 0.5 \text{ deg} \quad \varphi_0 = 0 \quad \Gamma_0 = 1.0 \text{ rad/s}$$

1) $\omega_{10} = 1.0$ rad/s
2) $\omega_{10} = 4.5$ rad/s } stable cases

3) $\omega_{10} = 1.5$ rad/s
4) $\omega_{10} = 2.0$ rad/s
5) $\omega_{10} = 3.0$ rad/s } unstable cases (21)

The above parameters, except ϑ_0, are the same as those in Ref. 4, from which one can draw trajectories in $\varphi - \vartheta$ plane by using Eq. (20) (see Fig. 3).

Figure 3 shows that if the initial values of nutational angle ϑ_0 are small, then ϑ will change in the small angular region for stable cases and will change into larger values for unstable cases. The nutational angle ϑ and spin angle φ in Fig. 3 have more obvious physical meanings than R and θ in Fig. 2 of Ref. 4. By comparing, one can see that the trajectory (5) in Fig. 2 of Ref. 4 is not correct. The reason is that it is not correct to replace I_{A3} by I to obtain Eq. (24) from Eq. (14b).

Conclusion

A new method for the nutational stability analysis of an asymmetric dual-spin spacecraft is presented. It is directly derived from the first-order differential equations of the system. The behavior of nutational motion is investigated with the aid of the energy integral of the system. The method can also be expanded to discuss nutational stability of a dual-spin spacecraft composed of two asymmetric bodies.

References

[1]Leimanis, E., *The General Problem of the Motion of Coupled Rigid Bodies About a Fixed Point,* Springer-Verlag, New York, 1965, pp. 207–232.

[2]Kane, T.R., "Solution of the Equations of Rotational Motion for a Class of Torque-Free Gyrostats," *AIAA Journal,* Vol. 8, June 1970, pp. 1141–1143.

[3]Cochran, J.E., Shu, P.H., and Rew, S.D., "Attitude Motion of Asymmetric Dual-Spin Spacecraft," *Journal of Guidance, Control, and Dynamics,* Vol. 5, Jan.-Feb. 1982, pp. 37–42.

[4]Tsuchiya, K., "Attitude Behavior of a Dual-Spin Spacecraft Composed of Asymmetric Bodies," *Journal of Guidance and Control,* Vol. 2, July-Aug. 1979, pp. 328–333.

[5]Liu, Y.Z., "A New Approach to the Motion of Rigid Body About a Fixed Point in Euler's Case," *Journal of Shanghai Mechanics,* Vol. 2, No. 3, 1981, pp. 52–55.

Sensor Failure Detection Using Generalized Parity Relations for Flexible Structures

Mathieu Mercadal*
Massachusetts Institute of Technology, Cambridge, Massachusetts

I. Introduction

GENERALIZED single-sensor parity relations (GSSPR) are an attractive method of fault detection and isolation (FDI) for large-scale systems such as space structures with a potentially great number of sensors.[1] GSSPR belongs, indeed, to the class of analytical redundancy methods that alleviate the need for replicating hardware components. Instead, a failure is indicated by the occurrence of a mismatch between the history of the actual sensor outputs and the history predicted using the analytical model.[2] GSSPR also leads to very simple isolation logic. Finally, generating the relations is particularly easy when the eigenstructure of the system is known, which is usually the case for flexible structures whose modeling is obtained via finite-element analysis. The method, unfortunately, suffers many shortcomings, one of which is a high sensitivity to modeling error and noise, as demonstrated in this paper by GSSPR test results obtained on the NASA Langley Spacecraft Control Laboratory Experiment (SCOLE). Part II of this paper treats GSSPR generation. Test results are presented in part III. Part IV concludes the paper.

II. Generalized Single-Sensor Parity Relations

Consider a discrete-time lumped parameter model describing the dynamics of a structure:

$$X(i+1) = A\ X(i) + B\ U(i) \tag{1}$$

where $X(i)$ is the state vector at time i, $U(i)$ contains all the command inputs, A and B are two constant coefficient matrices. A standard way to obtain such a model is through finite-element analysis.[3] Such a technique directly yields the continuous model in modal form. The discretization is a standard procedure.[4]

Received Oct. 8, 1987; revision received Jan. 26, 1988.

*Graduate Student, Research Assistant.